Supporting Information

Use of Gold Nanoparticles to Investigate the Drug Embedding and Releasing Performance in Biodegradable Poly(Glycerol Sebacate)

Yi-Kong Hsieh†, Chia-Teng Chang†, I-Hsin Jen‡, Fan-Chih Pu†, Shu-Huei Shen§,⊥, Dehui Wan‡, and Jane Wang†*

†Department of Chemical Engineering, National Tsing Hua University, Hsinchu 30013, Taiwan
‡Institute of Biomedical Engineering, National Tsing Hua University, Hsinchu 30013, Taiwan
§Department of Radiology, Taipie Veterans General Hospital, Taipei 11217, Taiwan
⊥School of Medicine, National Yang-Ming University, Taipei 11221, Taiwan

*corresponding author: Jane Wang; E-mail address: janewang@mx.nthu.edu.tw; postal address: NO.101, Section 2, Kuang-Fu Road, Hsinchu 30013, Taiwan

Number of Tables: 2
Number of Figures: 2
Number of pages: 3

Figure S1 demonstrated LA-ICP-MS methods applied in this study. Figure S1 (a) showed that laser moving with fixed speed and ablated on the surface of PGS-AuNPs composite material in a x to y-direction. To avoid overlap of the ablated sites between lines, the distance between each line in the y-direction is 150 μm apart, defined by the beam size of the laser. The laser parameters used in Figure S1 (b) were similar to those described in Figure S1 (a) but the analysis ran through cross-section of PGS-AuNPs composite material in a y to z-direction. The depth profiling is performed through repeated laser ablation on a single point of the sample, deepening in the z-direction, and was shown in Figure S1 (c).

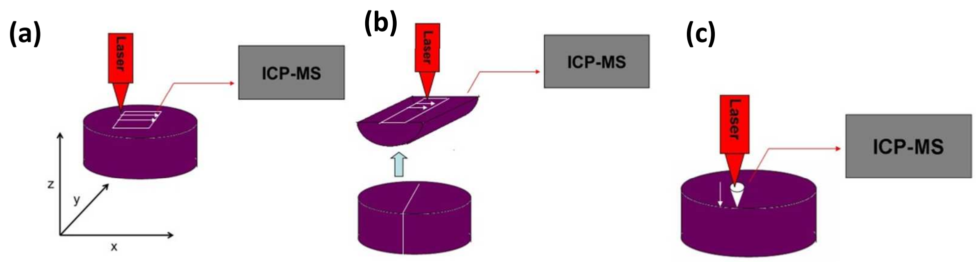

Figure S1. The illustrations of PGS-AuNPs composite material analysis via LA-ICP-MS with (a) surface mapping, (b) cross-section mapping and (c) depth profiling.

In Figure 1(b) and 5, PGS-AuNPs composite materials were ablated through depth profiling shown in Figure S1, and the depth of craters were measured through surface topography profilometer (Dektak 150, Veeco, USA), and the correlation between laser dwell time and crater depth were plotted in Figure S2. The results in Figure S2 showed that when laser ablated on PGS-AuNPs composite materials, the ablation efficiency was roughly 0.46 μm per ablation.

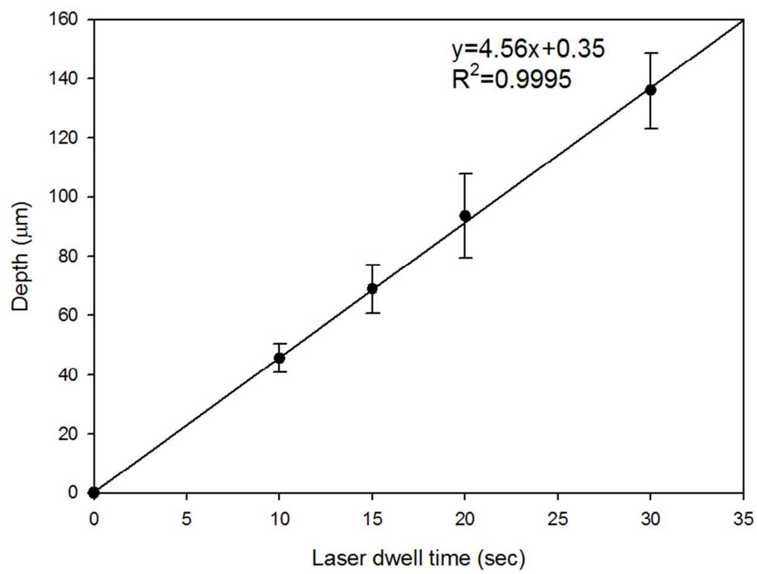

Figure S2. The correlation between laser dwell time and crater depth on PGS-Au composites.

As the resolution of LA-ICP-MS methods depends heavily on the data acquisition rate and the scan speed of the laser, the "spatial resolution" of the abovementioned LA-ICP-MS methods may be obtained through the division of scan speed (μm s^{-1}) by data acquisition rate (Hz) to describe the distance between each data point obtained. For example, the distance between data points in the x-direction of surface mapping was

$$100\ \mu m\ s^{-1} \div 1\ Hz = 100\ \mu m \qquad \text{Eq (S1)}$$

A full summary of the spatial resolution of three methods are shown in Table S1.

Table S1. Spatial resolution of LA-ICP-MS methods.

Distance between Data Acquisition	x-axis (μm)	y-axis (μm)	z-axis (μm)
Surface Mapping	100	150	-
Cross-Section Mapping	-	50	150
Depth Profiling	-	-	0.46

The diffusion condition of AuNPs in PGS matrix were further analyzed by using the self-diffusion model from one thin film toward both sides as shown in Eq (S2).

$$C_{A*} = \frac{M}{2\sqrt{\pi D_{A*} t}} exp\left[\frac{-x^2}{4D_{A*}t}\right] \quad \text{Eq (S2)}$$

M is the quantity of A* in moles per unit area of the joint, which acquired from the two times of integrated area below the curve in Figure 5. C_{A*}, t, and x are the concentration of AuNPs, length of degradation time, and distance of AuNPs diffused from the highest concentration observed in Figure 5, respectively. D_{A*} is the diffusion coefficient, which could be calculated through this equation. The pre C_A is the simulation results using the obtained D_{A*} value back into Eq (1). The R^2 is the correlation coefficient between pre C_A (the simulated values) and C_{A*} (the experimental results).

Table S2. Diffusion condition of the AuNPs in PGS films using the self-diffusion model

	7 Days	14 Days	21 Days	28 Days
D_{A*}(cm^2/s)	3.7179 x 10^{-14}	1.9862 x 10^{-14}	1.4520 x 10^{-14}	1.1259 x 10^{-14}
pre C_A(mM)	0.0636	0.0627	0.0542	0.0489
	0.0746	0.0727	0.0621	0.0558
	0.0844	0.0816	0.0690	0.0618
	0.0921	0.0887	0.0744	0.0665
	0.0970	0.0930	0.0778	0.0694
	0.0988	0.0946	0.0790	0.0704
C_{A*} (mM)	0.0548	0.0548	0.0548	0.0559
	0.0548	0.0564	0.0562	0.0588
	0.0556	0.0630	0.0625	0.0618
	0.0747	0.0796	0.0717	0.0641
	0.1111	0.0993	0.0818	0.0687
	0.1233	0.1140	0.0837	0.0702
R^2	0.6820	0.7842	0.8791	0.9351